The Egyptian Journal of Hospital Medicine (January 2023) Vol. 90, Page 1274-1283

# Antimicrobial and Antibiofilm Activity of Gold Nanoparticles Biosynthesized Using *Acinetobacter Baumannii* Isolated from Wounds and Burns

**Intesar H. Al-Abdeli* and Esam J. Al-Kalifawi**
Department of Biology, College of Education for Pure Science Ibn -Al- Haitham,
University of Baghdad, Baghdad, Iraq
***Corresponding author: Intesar H. Al-Abdeli, Mobile:** (+20) 01140292959,
**Email:** Intessar.Hameed1102a@ihcoedu.uobaghdad.edu.iq"

## ABSTRACT

**Background:** Due to their biological and physiochemical characteristics, metal-based nanoparticles show promise as antimicrobials and therapeutic agents.

**Aim:** This study aimed to biosynthesize AuNPs from *A. baumannii* broth and test their antibacterial and ant-virulence properties.

**Materials and methods:** UV-vis, FTIR, XRD, TEM, FESEM and AMF were used to analyze biosynthesized gold nanoparticles. The well method diffusion assay was utilized to determine Ab-AuNPs' antibacterial activity against five bacterial strains. Microtiter plate was used to study the effect of Ab-AuNPs on biofilm formation in five bacterial isolates.

**Results** Biosynthesized Ab-AuNPs feature 574 nm UV-Visible SPR bands. Ab-AuNPs biosynthesized at 3321.42, 2823.79, 2144.84, 1631.78 $cm^{-1}$, amide III, polypeptides, and proteins form these bands. *A. baumannii* polypeptides capped AuNPs. The peaks at 111, 200, 220, and 311 reflect the 2 Bragg angles 38.18°, 44.51°, 64.80°, and 77.72°. Debye Scherrer's equation calculated Ab-AuNPs crystallite size (26.82 nm). Biosynthesized Ab-AuNPs were 20-90 nm in size, with an average of 66 nm. AFM measures Ab-AuNP shape. AFM images show Ab-AuNP size distribution. Ab-AuNPs averaged 63.82 nm. The diameter of the inhibitory zone decreases with Ab-AuNP concentration. Biosynthesized Ab-AuNPs inhibited biofilm formation in five bacterial strains.

**Conclusions:** We concluded that the biosynthesized Ab-AuNPs have effective antibacterial and antibiofilm activity that could enhance the action of existing antibiotics and could be a therapeutic agent.

**Keywords:** Gold nanoparticles, Acinetobacter baumannii, Antibiofilm activity, Antibacterial activity.

## INTRODUCTION

*Acinetobacter baumannii* is gram-negative strictly aerobic, nonmotile, encapsulated, non-lactose-fermenting and non-fastidious coccobacillus [1, 2]. *A. baumannii* is very adept at living in hospital environments. Because it can form biofilms, it can cause infections that last for a long time. *A baumannii* is extensively present in natural surroundings and constantly accompanying aquatic environments as an opportunistic bacterial pathogen that precipitously increases nosocomial infections [3, 4].

The necessity for nanoparticle biosynthesis has increased. As a result, researchers have turned to microorganisms and plant extracts to create nanoparticles [5].

Gold nanoparticles (AuNPs) have an advantage because they are high in the surface area-to-volume ratio, improved biocompatibility, and low in the toxicity. So, AuNPs is an important bionanotechnology tool. As the core magnitude grows from 1-100 nm, gold NPs with surface plasmon resonance show a range of hues in an aqueous solution, including red, brown, orange, and purple [6]. The enormous potential of microorganisms as eco-friendly and economical tools, Due to a variety of reductase enzymes, changing metal salts into metal nanoparticles narrowly to a lesser degree of polydispersity, microorganisms can accumulate and detoxify heavy metals [7]. The cell membrane bactericidal destruction, interference with enzyme pathways, microbial cell wall alteration, and nucleic acid synthesis inhibition are just a few of NPs' antimicrobial effects [8]. Many NPS size and surface chemistry of the govern their antibacterial properties. Bacterial biofilm is particularly resistant to antibiotic treatment [9].

This ascribes to the spread of resistance indicators and the extracellular polymeric matrix's ability to obstruct drug transport [10]. Biosynthesized AuNPs have been shown to have antibiofilm activity against harmful bacteria [11].

## MATERIALS AND METHODS

### Collection of pathogens bacteria

We collected twenty-five Multiple antibiotic-resistant isolates from a burn and wound. The current study was conducted at Yarmouk Teaching Hospital and Baghdad Medical City laboratories in March 2022. They included five strains of bacteria; *Acinetobacter baumannii, Pseudomonas aeruginosa, Staphylococcus epidermidis*, and *Escherichia coli*. Standard biochemical tests and diagnostics identified these isolates and, finally, the Vitek 2 Compact system [12].

### Biosynthesis of gold nanoparticles"

The modified procedure of **Sabir *et al.*** [13] was used in the biosynthesis of AuNPs. Two milliliters, four milliliters, six milliliters, eight milliliters, and ten milliliters of *A. baumannii* broth culture mixed with ten milliliters of stock solution of $HAuCl_4.4H_2O$ separately in a flask and heated at 50°C for 30 minutes on a



Received: 03/08/2022
Accepted: 04/10/2022

magnetic hotplate stirrer. We added ionized water to the volume of 15 ml. The resulting solution was put into a tube and in the ultrasonic bath for 30 minutes.

The solution changed color from bright yellow to yellowish-orange after the appearance of red dots on the sides of the transparent tube inside the ultrasonic bath device. The steps are repeated each time; two ml of the bacterial broth culture is added to the gold salt solution while maintaining the other conditions, such as gold salt solution concentration, temperature, time, and a constant pH value, to go to the end of these steps an orange-colored solution that turns into a light purple and finally a darker purple that indicated synthesis of the gold nanoparticles.

**Characterization of Ab-AuNPs**

We examined the AuNP characterization biosynthesized by *A. baumannii* broth culture by Ultra Violate-Visible (UV-Vis) Spectroscopy, Atomic Force Microscope (AFM), Spectroscopy, Field Emission Scanning Electron Microscope (FE-SEM), Fourier Transforms Infrared (FTIR) Transmission Electron Microscope (TEM) and X-Ray Diffraction (XRD) analysis.

**Determination of Antibacterial Activity of Ab-AuNPs:** The Ab-AuNPs antibacterial activity of *A. baumannii* broth culture was determined according to **Bahjat *et al.* [14].**

**Determination of antibiofilm activity of Ab-AuNPs:**

The antibiofilm activity of Ab-AuNPs against five types of bacteria, three belonging to Gram-negative bacteria and two bacteria belonging to Gram-positive bacteria, were determined using one method the Micro-titter plate method**.**

The micro-titter plate method was used according to **[15].**

**Ethical approval**

Ethical and Scientific Committee of the Department of Biology in in the College of Education for Pure Science, Ibn-Al-Haitham University, Baghdad, Iraq agreed to give their permission to the cross-sectional study that was conducted with approval number: RECACPUB-3102020D. Prior to data collection, signed consent was obtained from each participant. Out of 25 participants met the study.

***Statistical analysis***

We conducted the statistical analysis of the data by GraphPad Prism 6, and the findings expressed as mean ± SD of three replicates for each experiment **[16].**

**RESULTS**

Figure (1) showed color change from yellow to dark violet, evidence of the biosynthesis of Ab-AuNPs using *A. baumannii* broth culture.

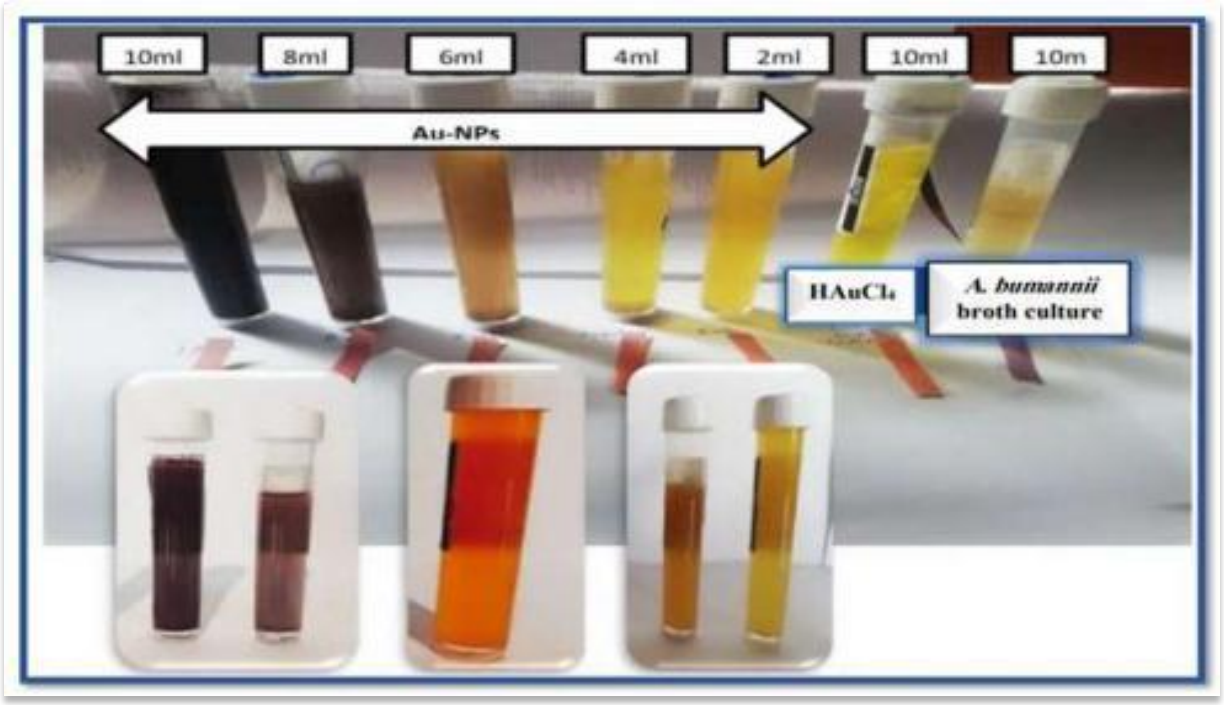


**Figure (1):** Exhibit gold nanodots in suspension. Particle sizes and shapes cause color differences.

**UV-Visible analysis**

Figure (2) showed the UV-Visible spectrum of Ab-AuNPs biosynthesized utilizing *A. baumannii* broth culture. Surface plasmon resonance (SPR) bands of about 574 nm were seen in the UV-Visible spectra of Ab-AuNPs.

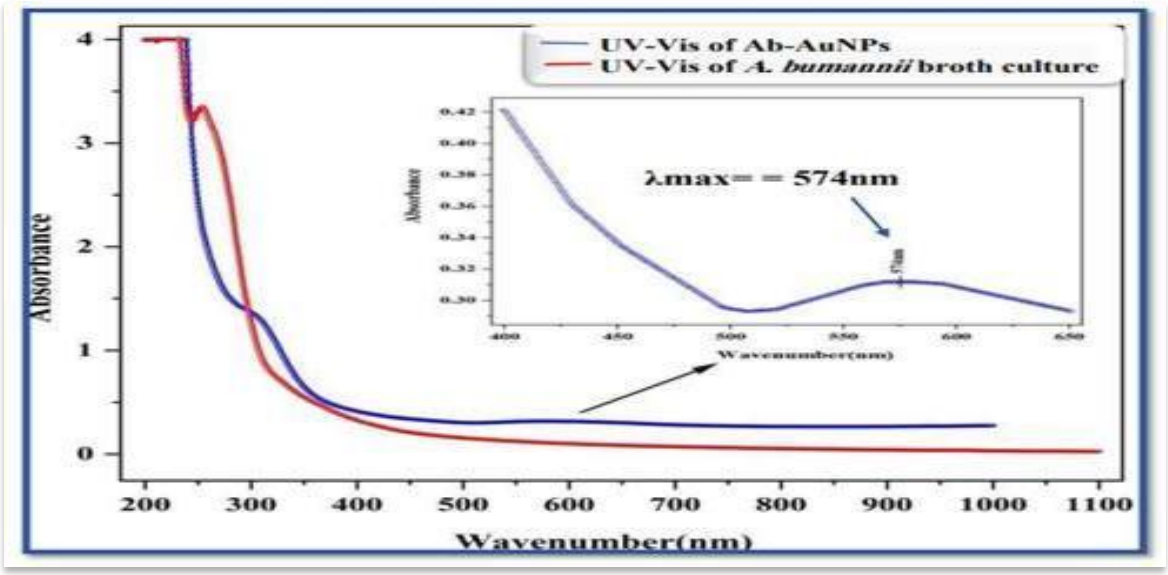


**Figure (2):** UV-Vis spectrum of Ab-AuNPs colloidal and *A. baumannii* broth culture.

**Fourier transforms infrared spectroscopy analysis"**

FT-IR spectra of Ab-AuNPs in figure (3) demonstrated the main peaks at 3321.42, 2823.79, 2144.84 and 1631.78 $cm^{-1}$. The broad peak at 3321.421$cm^{-1}$ is linked to O–H stretching*vibration of hydrogen-bonded alcohols. It is also linked to phenol, and associated with N-H stretching of amines or amides. In alkanes, aldehyde, the C = H stretch and in corrosive carboxylic C – H stretch showed up separately at 2823.79$cm^{-1,}$ while at 1631.78 $cm^{-1}$ with the C=O bond stretching vibrations. Identified sharp peaks in the range of 578.64–748.38 $cm^{-1}$ refer to the vibration of Ab-AuNPs. This confirms the effective formation of Ab-AuNPs **(17).**

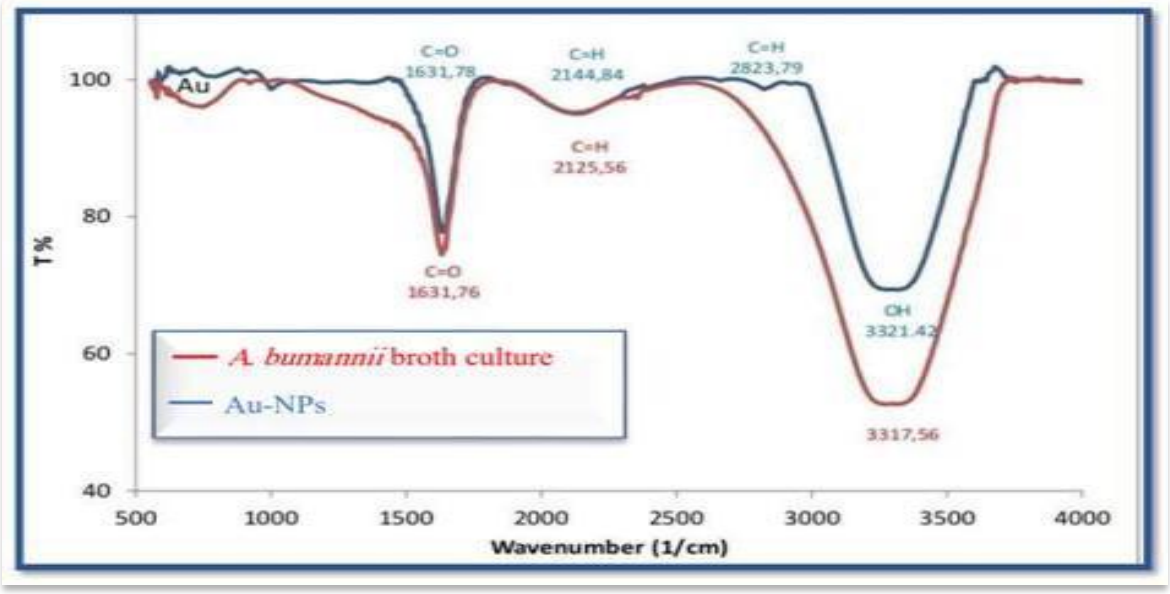


**Figure (3):** FT-IR spectrum of (read) *A. baumannii* broth culture and (blue) the Ab-AuNPs colloidal.

***XRD analysis***

Reflections with 2θ of the Bragg angles of 38.18°, 44.51°, 64.80°, and 77.72° correspond to the principal peaks found at 111, 200, 220, and 311, as shown in figure (4). As shown below, the tested sample is indeed AuNPs of very high purity. According to the Debye-Scherrer equation, the arranged Ab-AuNP mean crystallite size is 26.82 nm **(18).**

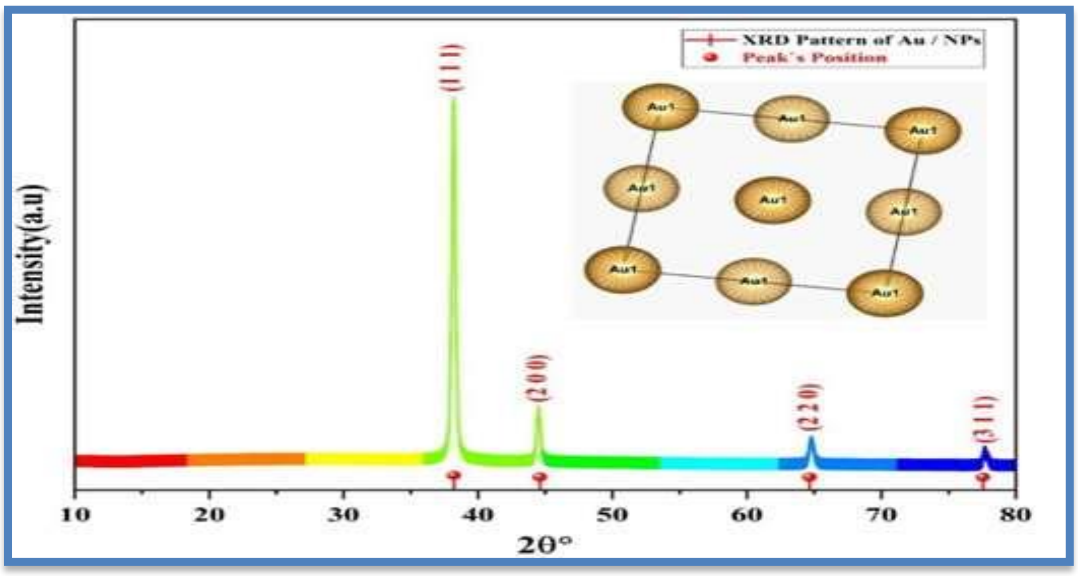


**Figure (4):** XRD of Ab-AuNPs biosynthesized using *A. baumannii* broth culture.

D = $K\lambda\beta COS\theta$

Which elaborates on the link between crystallite size and XRD peak broadening in which D is the nanoparticle mean diameter, Scherrer constant K=0.9, λ is the X-ray photon source (0.15406 nm) wavelength in which θ denotes Bragg's angle.

**Transmission Electron Microscope (TEM) Examination**

"The size of Ab-AuNPs ranged between 20-90 nm, with 66 nm diameters in average as in figure (5). The semi-spherical Ab-AuNPs are generated at the start of the reaction. Subsequently, they are aggregated together due to a large amount of reducing factor in the *A. baumannii* broth culture. In addition to spherical rectangular, triangular, pentagonal, cylindrical, irregular, and polymorphic".

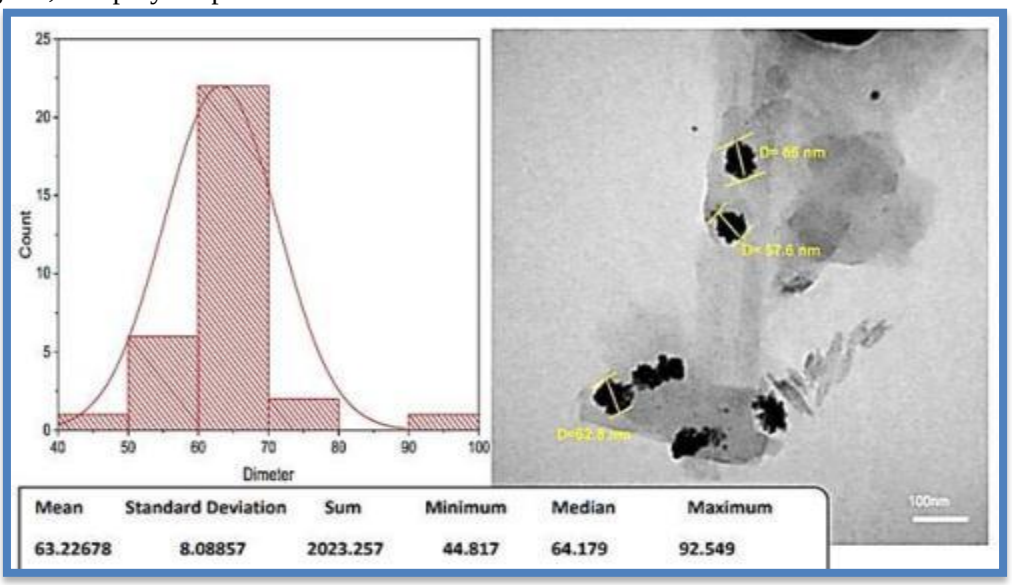


**Figure (5):** TEM image of biosynthesized AuNPs using *A. baumannii* broth culture, (a) Average diameters of gold nanoparticles, (b) diverse shapes.

**FESEM**

The Ab-AuNPs have a spherical shape and the aggregation is high1as in figure (6), and the Ab-AuNPs size ranged between 66-363 nm.

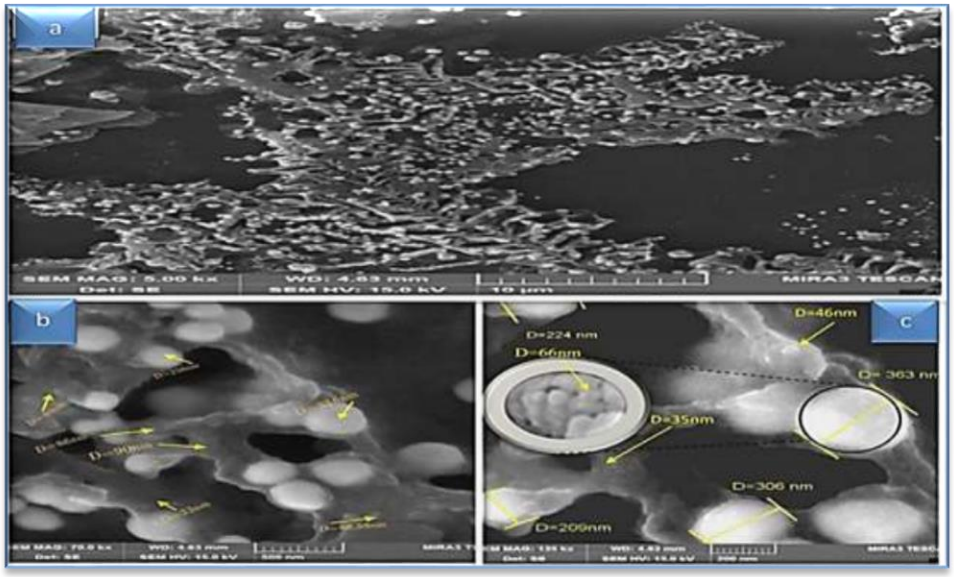


**Figure (6):** FESEM images of biosynthesized Ab-AuNPs using *A. baumannii* broth culture, a, b, c shows shapes of Ab-AuNPs.

**"AFM Analysis"""**

The 2D and 3D AFM images reveal the spread out of the Ab-AuNPs sizes. After two months of making AuNPs, the AFM sample on the slide did not show any agglomeration or aggregation, which indicated that the Ab-AuNPs made are very stable. The Ab-AuNPs particle from 15 to 125 nm, and their average length was 63.82 nm (Figure (7).

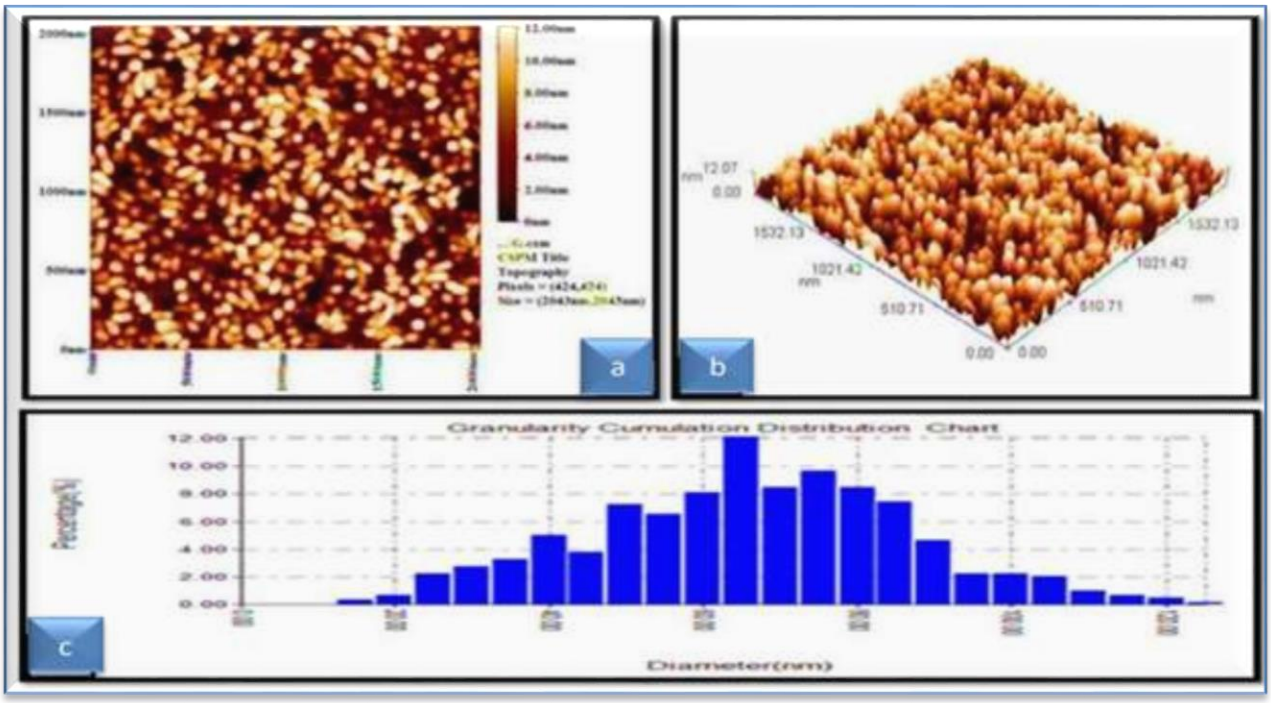


**Figure (7):** AFM images of biosynthesized Ab-AuNPs using *A. baumannii* broth culture, (a) Two-Dimensional, (b) Three-Dimensional, and (c) Average particle size.

The inhibition zone was 34, 31, 35, 30, and 33mm for *A. bumannii* No.66, *S. aureus* No.48, *P. aeruginosa* No.29, *S. epidermidis* No.20, and *E. coli* No.10 in 500 µg/ml concentration of Ab-AuNPs. While, the inhibition zone size was 29, 22, 17, 15, and 19 mm for *A. bumannii* No.66, *S. aureus* No.48, *P. aeruginosa* No.29, *S. epidermidis* No.20, and *E. coli* No.10 in the 62.5 µg/ml Ab-AuNPs concentration (table 1 and figures 9-13).

**Table1.** Antimicrobial activity of different concentrations of Ab-AuNPs

| Isolates | Inhibition zone/mm | | | | |
|---|---|---|---|---|---|
| | Ab-AuNPs Concentrations | | | | |
| | Control/0.0 µg/ml. | 62.5 µg/ml. | 125 µg/ml. | 250 µg/ml. | 500 µg/ml. |
| *A. bumannii* No. 21,66,20,10,11 | 6.180±0.188* | 29.53±1.112* | 32.36 ±1.08* | 35.37 ±0.664* | 34.91 ±1.050* |
| *S. aureus* No. 48,17,46,2,15 | 6.040±0.11* | 22.64±2.76* | 23.43 ±2.43* | 29.40 ±2.61* | 31.10 ±2.403* |
| *P. aeruginosa* No. 16,23,19,27,29 | 6.160±0.11* | 17.25±0.988* | 22.29 ±0.847* | 31.79 ±1.931* | 35.89 ±1.780* |
| *S. epidermidis* No. 10,20,18,7,39 | 6.140±0.186* | 15.43±1.133* | 22.57 ±0.948* | 27.16 ±0.929* | 30.29 ±0.650* |
| *E. coli* No. 10,12 ,13,8,19 | 6.220±0.171* | 19.04±1.146* | 26.91 ±1.145* | 29.93 ±1.468* | 33.22 ±1.472* |

*These numbers represent the mean numbers of five isolates of each bacterial type

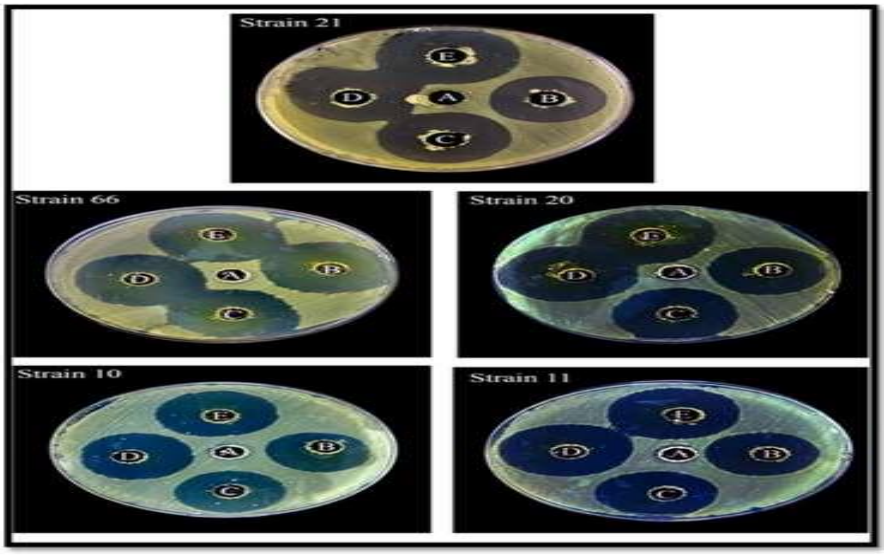


**Figure (9):** Ab-AuNP antibacterial process against five isolates of *A. bumannii*.

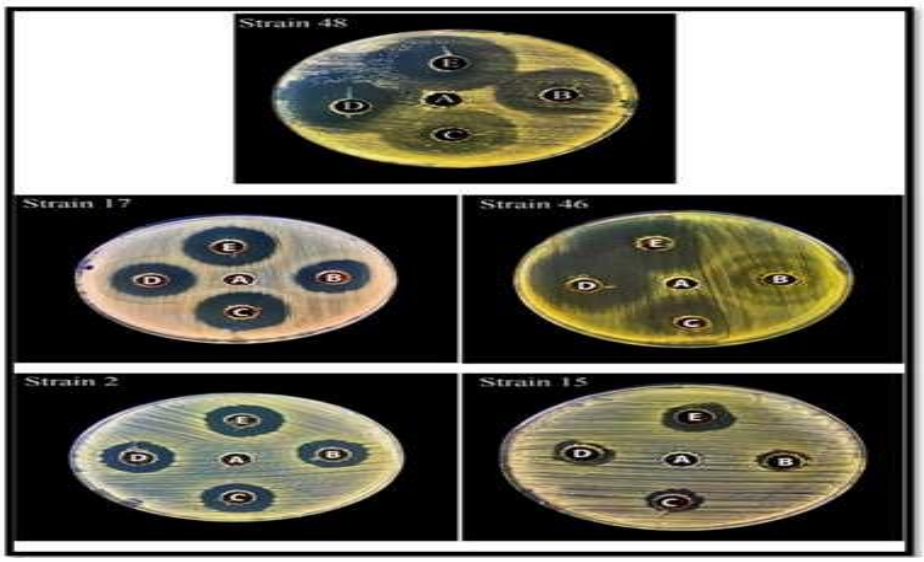


**Figure (10):** AuNP antibacterial process against the same five isolates of S. aureus at the same sizes

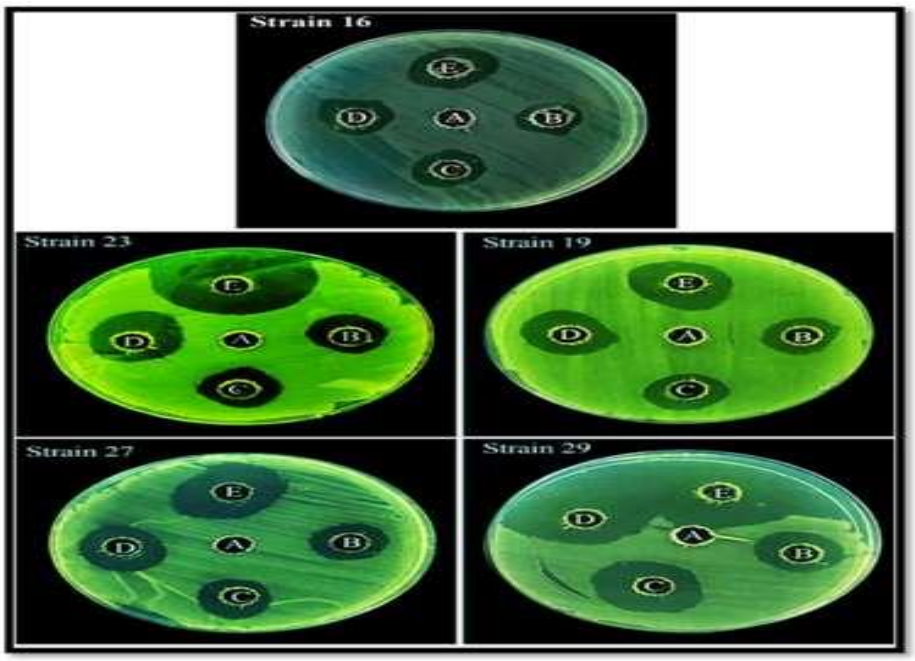


**Figure (11):** Antibacterial activity of Ab-AuNPs against five isolates of *P. aeruginosa* at the same sizes

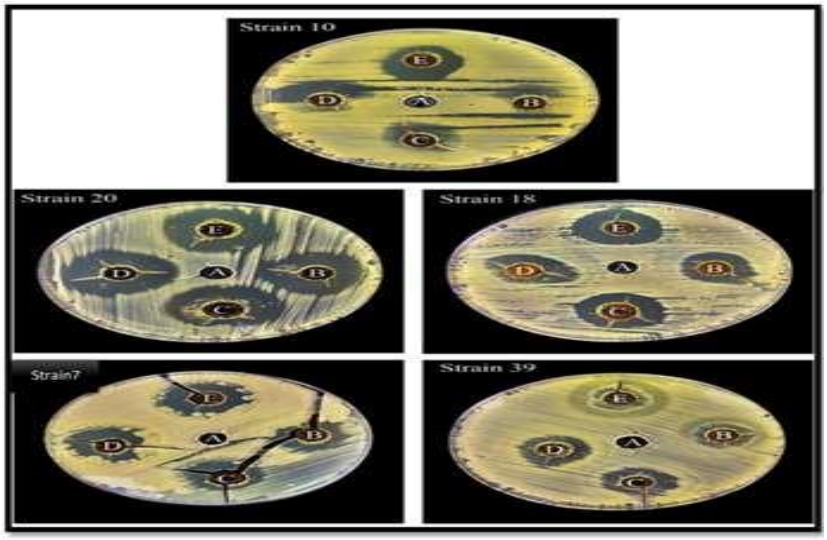


**Figure (12):** Antibacterial activity of Ab-AuNPs against five isolates of S. epidermidis at the same sizes

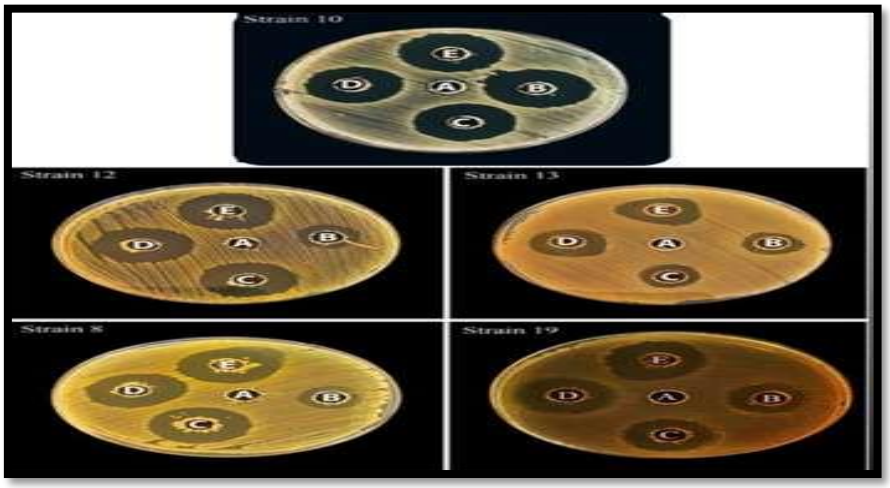


**Figure (13):** AuNP antibacterial process against five isolates of *E. coli*.

**Determination of antibiofilm activity of Ab-AuNPs:** This study showed that multiple antibiotic-resistant bacterial strains have a high degree of biofilm formation in a significant manner. Using gold nanoparticles in one method showed it has effective antibiofilm activity.

**Micro-titter plate method:** The results showed the reduced optical density of wells containing different concentrations of Ab-AuNPs compared to the well optical density with no Ab-AuNPs (Figure 14).

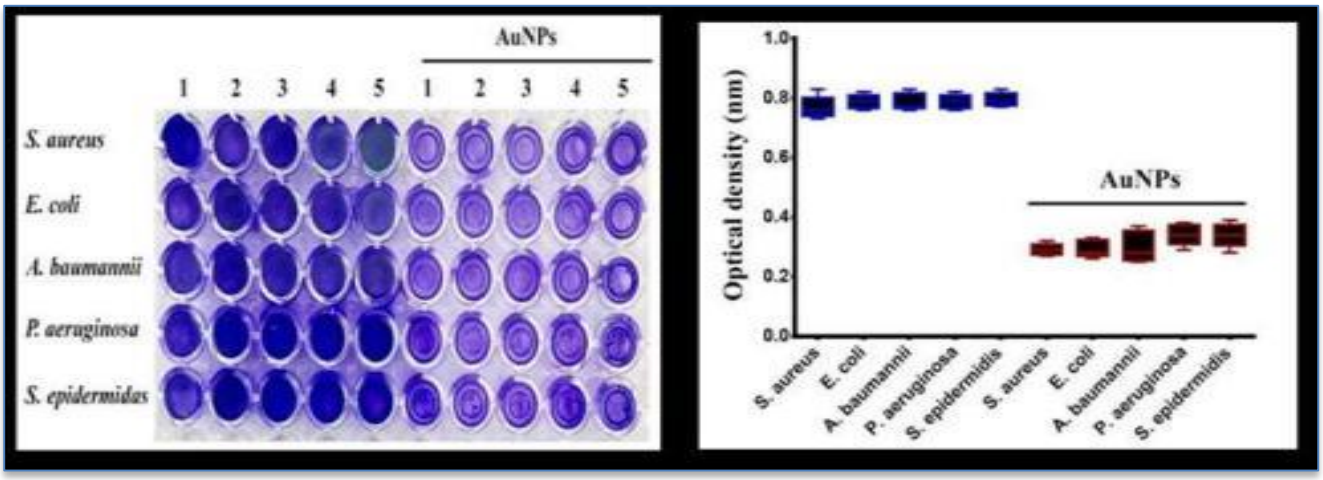


**Figure (14):** The antibiofilm activity of Ab-AuNPs in Gram-negative and Gram-positive bacteria using the Micro-titter plate.

---

## DISCUSSION

The current study is the first in which the Ab-AuNPs were biosynthesized using *A. baumannii* broth culture mixed with the gold solution. Broth culture contains the metabolism materials of bacterial cells, such as peptides, polysaccharides, amino acids, proteins, and enzymes. The Ab-AuNPs biosynthesis included these materials can reduce and cape agents. In broth culture, the color change from light yellow to deep purple showing that Ab-AuNPs had formed and were proof of synthesis. These findings are consistent with prior research that suggested metal biotransformation may entail a group. of,cape.proteins. or-peptides. It also entails reductases, quinines, cytochromes, phytochelatins, or electron shuttles for reducing different metals and metal oxides **(19).** This study used several volumes of broth culture with a fixed volume of gold solution. The color change rises with the risen broth culture added volume, indicating that the reducing and capping agents for AuNPs increased with the increase in the broth culture added for the reaction. These findings are in agreement with **Ali *et al.* (20).**

The UV-Visible spectra showed that Ab-AuNPs have surface plasmon resonance (SPR) bands around 574 nm. These findings are in agreement with **Swami *et al.* (21)** in which the UV-Visible spectra of AuNPs within the apparent absorbance band area was 500 nm-600 nm.

The Ab-AuNPs biosynthesized by *A. baumannii* broth culture were submitted to FTIR analysis to uncover the biomolecules involved in the solution's nanoparticle stabilization. The AuNPs synthesized by *A. baumannii* broth culture yielded strong bands at 3321.42, 2823.79, 2144.84 and 1631.78) $cm^{-1}$. These bands1correspond to the amide III, polypeptides, and proteins and"are consistent with previous reports" **(22).**

The polypeptides in the *A. baumannii* broth culture served as capping agents in AuNPs. Identified sharp peaks in the range of 578.64–748.38 $cm^{-1}$ refer to the AuNPs' vibration. As a result, AuNPs were successfully generated. The XRD spectrum has four main peaks that match Bragg's reflection of AuNPs found in a previous study that used bacteria and yeast extracellular and intracellular culture supernatant **(23).** The main peaks found at 111, 200, 220, and 311 correspond to reflections with 2θ values of the Bragg angles of 38.18°, 44.51°, 64.80°, and 77.72°, respectively. These results show that the tested material is AuNPs and is very pure. The Debye Scherrer equation is used to show the mean crystallite size of Ab-AuNPs in an arrangement of 26.82 nm. Our current results align with past research that used plant extracts and biological methods to make AuNPs, yeast, and bacteria **(24).**

TEM (Transmission Electron Microscope) examination showed that the size of AuNPs biosynthesized using the *A. baumannii* broth culture ranged between 20-90 nm, with a mean of 66 nm. They have a semi-spherical shape and are clustered together. These results agree with several previous studies **(25).**

FESEM results showed that the shape and size of biosynthesized AuNPs using the *A. baumannii* broth culture were close to the transmission electron microscopy results. These results agree with another study **(26).**

The biosynthesized Ab-AuNPs size and shape by the *A. baumannii* broth culture were calculated by atomic force microscope (AFM). The results showed the 2D and 3D AFM images with the size distribution of AuNPs that goes with them. The Ab-AuNPs particle size was 15-125 nm, with an average length of 63.82 nm. These results agree with another study **(27).** At the same time, another study synthesized AuNPs with

different sizes [28]. This difference in length may be due to the methods of synthesis, changes in the type of bacteria or plant extract, and the differences in conditions chosen for synthesis.

The antimicrobial activity results showed that the diameter of the inhibition zone decreases with a drop in the concentration of Ab-AuNPs. These results agree with previous study [29], which mentioned that AuNPs have antibacterial activity against *A. baumannii* and the inhibition zone's diameters decreased with Ab-AuNPs concentration. The variation in the effect of AuNPs on different strains of *S. aureus* is due to the AuNPs' action via their interactions with bacterial cells.

The1 nanoparticle decommissioning ions interact with the -SH (thiol) group of the transport protein that emanates from the bacterial cell membrane disrupting permeability and functions of cellular respiration or interfering with the bacterial electron transport chain elements, resulting in bacterial cell death [30].

one technique was used to study the effect of Ab-AuNPs on biofilm formation in five bacterial isolates, the Micro-titter plate method. The results proved the efficacy of both forms of Ab-AuNPs biosynthesized A. baumannii broth culture in inhibiting biofilm production in five isolates. These results agree with another study [31].

## CONCLUSION

We concluded that the biosynthesized Ab-AuNPs have effective antibacterial and antibiofilm activity that could enhance the action of existing antibiotics and could be a therapeutic agent.

## ACKNOWLEDGMENTS

We submit1 our thanks and appreciate Director 1of Yarmouk Teaching Hospital and Baghdad1 Medical City for providing us with isolates of MDR1 bacteria. Also, we thank and appreciate the staff of the Department of Biology at the College of Education1for Pure Sciences, Ibn Al-Haytham for their*encouragement.

- **Conflict of interest:** The authors declared no conflict of interest.
- **Sources of funding:** This research did not receive any specific grant from funding agencies in the public, commercial, or not-for-profit sectors.

## REFERENCES

1. **Baumann P, Doudoroff M, Stanier R (1968):** A study of the Moraxella group II. Oxidative-negative species (genus Acinetobacter). Journal of Bacteriology, 95 (5): 1520-1541.
2. **Özgür Ö, Aksaray N (2014):** Acinetobacter Infections and Treatment/Acinetobacter Enfeksiyonlari ve Tedavisi. Cocuk Enfeksiyon Dergisi, 8 (1): 28-39.
3. **Prashanth K, Badrinath S (2006):** Nosocomial infections due to Acinetobacter species: Clinical findings, risk and nttentent prognostic factors. Indian Journal of Medical Microbiology, 24 (1): 39-44.
4. **Al-Mathkhury F, Al-Dhamin S, Al-Taie L (2016):** Antibacterial and antibiofilm activity of flaxseed oil. Iraqi Journal of Science, 57 (2): 1086-1095
5. **Al-Kalifawi J, Al-Obodi E, Al-Saadi M (2018):** Characterization of Cr2O3 nanoparticles prepared using different plant extracts. Academia J. Agricult. Res., 6 (5): 26- 32.
6. **Yeh C, Creran B, Rotello M (2012):** Gold nanoparticles: preparation, properties, and applications in bionanotechnology. Nanoscale, 4 (6): 1871-1880.
7. **Kim S, Kuk E, Yu K *et al.* (2007):** Antimicrobial effects of silver nanoparticles. Nanomedicine: Nanotechnology, biology and medicine, 3 (1): 95-101.
8. **Al-Kalifawi J, Al-Azzawi J, Hassan F (2018):** Biosynthesis of silver nanoparticles using Al-Ankabut's home extract and its antimicrobial activity. Academia J. Agricult. Res., 6 (5): 033-046.
9. **Herdt J, Feng H (2009):** Aqueous antimicrobial treatments to improve fresh and fresh-cut produce safety. Microbial safety of fresh produce, 14 (3): 167-190.
10. **Franci G, Falanga A, Galdiero S *et al*. (2015):** Silver nanoparticles as potential antibacterial agents. Molecules, 20 (5): 8856-8874.
11. **Vinoj G, Pati R, Sonawane A *et al.* (2015):** In vitro cytotoxic effects of gold nanoparticles coated with functional acyl homoserine lactone lactonase protein from Bacillus licheniformis and their antibiofilm activity against Proteus species. Antimicrobial agents and chemotherapy, 59 (2): 763-771.
12. **Frebourg B, Nouet D, Lemee L *et al.* (1988):** Comparison of ATB staph, rapid ATB staph, Vitek, and E- test methods for detecting oxacillin heteroresistance in Staphylococci possessing mecA. J. Clin. Microbiol., 36: 52-57.
13. **Sabir S, Zahoor A, Waseem M *et al.* (2020):** Biosynthesis of ZnO nanoparticles using bacillus subtilis: characterization and nutritive significance for promoting plant growth in Zea mays. L. Dose-Response, 18(3): 219-233.
14. **Bahjat H, Ismail A, Sulaiman M *et al.* (2021):** Magnetic field-assisted laser ablation of titanium dioxide nanoparticles in water for anti-bacterial applications. Journal of Inorganic and Organometallic Polymers and Materials, 13 (2): 1-8.
15. **Hochbaum I, Kolodkin-Gal I, Foulston L *et al.* (2011):** Inhibitory effects of D-amino acids on Staphylococcus aureus biofilm development. Journal of Bacteriology, 193 (20): 5616-5622.
16. **Younis M, Abdel-Aziz M, Yosri M (2019):** Evaluation of some biological applications of Pleurotus citrinopileatusand Boletus edulis fruiting bodies. Current Pharmaceutical Biotechnology, 20 (15): 1309-1320.
17. **Ismail H, Saqer M, Assirey E *et al.* (2018):** Successful green synthesis of gold nanoparticles using a Corchorus olitorius extract and their antiproliferative effect in cancer cells. International journal of molecular sciences, 19 (9): 612-622.
18. **Kroon E (2013):** Nanoscience and the Scherrer equation versus the Scherrer-Gottingen equation'. South African Journal of Science, 109(5): 1-2.
19. **Suresh K, Pelletier A, Wang W *et al.* (2011):** Biofabrication of discrete spherical gold nanoparticles using the metal-reducing bacterium Shewanella oneidensis. Acta Biomaterialia, 7(5): 2148-2152.
20. **Ali S, Perveen S, Shah R *et al.* (2020):** Bactericidal

potentials of silver and gold nanoparticles stabilized with cefixime: a strategy against antibiotic-resistant bacteria. Journal of Nanoparticle Research, 22(7): 1-12.

21. **Swami A, Mittal S, Chopra A *et al.* (2018):** Synthesis and pH-dependent assembly of isotropic and anisotropic gold nanoparticles functionalized with hydroxyl-bearing amino acids. Applied Nanoscience, 8 (3): 467-473.
22. **Abdel-Raouf N, Al-Enazi M, Ibraheem B (2017):** Green biosynthesis of gold nanoparticles using Galaxaura elongate and characterization of their antibacterial activity. Arabian Journal of Chemistry, 10: 3029-3039.
23. **Singaravelu G, Arockiamary S, Kumar G *et al.* (2007):** A novel extracellular synthesis of monodisperse gold nanoparticles using marine alga, Sargassum wightii Greville. Colloids and surfaces B: Biointerfaces, 57 (1): 97-101.
24. **Sharma N, Pinnaka K, Raje M *et al.* (2012):** The exploitation of marine bacteria for the production of gold nanoparticles. Microbial cell factories, 11 (1): 1-6.
25. **Luzala M, Muanga K, Kyana J *et al*. (2022):** A Critical Review of the Antimicrobial and Antibiofilm Activities of Green-Synthesized Plant-Based Metallic Nanoparticles. Nanomaterials, 12 (11): 841-862.
26. **Owain N, Al-Saeedi S, Abed A (2017):** Biosynthesis of gold nanoparticles using yellow oyster mushroom Pleurotus cornucopiae var. citrinopileatus. Environmental nanotechnology, monitoring & management, 8: 157-162.
27. **Aljabali A, Akkam Y, Al Zoubi S *et al*. (2018):** Synthesis of gold nanoparticles using leaf extract of Ziziphus and their antimicrobial activity. Nanomaterials, 8 (3): 174-185.
28. **Sun B, Hu N, Han L *et al.* (2019):** Anticancer activity of green synthesized gold nanoparticles from Marsdenia tenacissima inhibits A549 cell proliferation through the apoptotic pathway. Artificial cells, nanomedicine, and biotechnology, 47 (1): 4012-4019.
29. **Cumberland A (2011):** Synthesis and environmental chemistry of silver and iron oxide nanoparticles (Doctoral dissertation, University of Birmingham). https://etheses.bham.ac.uk/id/ eprint/ 1736/
30. **Ghafoor A, Yas M, Saeed A (2019):** The Properties of Nano-Gold Particles Synthesized by Ascorbic Acid with Acacia Gum and Sodium Hydroxide as Stabilizers. Iraqi Journal of Science, 60(10): 2149-2155.
31. **Rajput N, Bankar A (2017):** Bio-inspired gold nanoparticles synthesis and their anti-biofilm efficacy. Journal of Pharmaceutical Investigation, 47 (6): 521-530.